J|A|C|S
ARTICLES
Published on Web 12/15/2005

On the Role of Tetramethylammonium Cation and Effects of Solvent Dynamics on the Stability of the Cage-like Silicates $Si_6O_{15}^{6-}$ and $Si_8O_{20}^{8-}$ in Aqueous Solution. A Molecular Dynamics Study

Stavros Caratzoulas,*,† Dionisis G. Vlachos,† and Michael Tsapatsis‡

Contribution from the Department of Chemical Engineering, University of Delaware, Newark, Delaware 19716, and Department of Chemical Engineering and Materials Science, University of Minnesota, 421 Washington Avenue SE, Minneapolis, Minnesota 55455

Received September 6, 2005; E-mail: caratzou@che.udel.edu

Abstract: We have undertaken explicit solvent molecular dynamics simulations to investigate the preferential stabilization of the silicate octamer $Si_8O_{20}^{8-}$ over the hexamer $Si_6O_{15}^{6-}$ in relation with the ability of tetramethylammonium (TMA) to form an adsorption layer around these cage-like polyions. We have found that the hexamer cannot support such a layer and as a result is vulnerable to hydrolysis. The dynamics of TMA desorption off the surface of the hexamer is investigated in connection with the solvent dynamics. We have studied the energetics of this preferential stabilization by calculating the relative change in the free energies of formation between the complexes $Si_8O_{20}^{8-}$·8TMA and $Si_6O_{15}^{6-}$·6TMA and found the former to be more stable by 70 kcal/mol. We also find that the energetics are consistent with experimental data, suggesting that the hexamer is a long-lived metastable species. Furthermore, we have studied the solvent structure and dynamics in the vicinity of both the bare polyions and their complexes with TMA. We have found that, as anticipated, both the octamer and the hexamer participate in hydrogen bonds with the water molecules, regardless of whether a TMA adsorption layer exists or not. In fact, we find that the presence of a TMA adsorption layer has a rather profound effect on the stability of these hydrogen bonds—it increases their lifetime by at least a factor of 2 relative to that of the hydrogen bonds between water and the bare polyions.

1. Introduction

Zeolite crystallization assisted by organic cations, typically tetraalkylammonium cations (TAA), involves complex solution and colloidal chemistry. A host of modern analytical techniques have been employed in studies aimed at elucidating the molecular processes that take place. A detailed understanding of the atomic scale mechanisms of the template-assisted formation of these materials is a prerequisite before we are able to develop rational strategies for their design, which remains chiefly an empirical endeavor and usually requires very costly trial-and-error modifications to reagents and conditions.

Motivated by the experimental (^{29}Si NMR) work of Kinrade et al.[1,2] on the formation of the cage-like species $Si_8O_{20}^{-8}$ and $Si_6O_{15}^{-6}$, we recently reported[3] results, obtained from molecular dynamics simulations, strongly suggesting that the stability of the cage-like, cubic octamer $Si_8O_{20}^{-8}$ (also referred to as "double four-ring" or Q_8^3) in aqueous solution is subject to the ability of the $(CH_3)_4N^+$ cations (TMA) in the solution to adsorb onto the surface of the cubic octamer. Formation of Q_8^3 has been observed to take place only at high TMA:SiO_2 ratios. Our simulations similarly showed that TMA cannot adsorb at the surface of Q_8^3, at low TMA concentrations, and only at high (2:1) TMA:SiO_2 ratios do we see full TMA coordination around the cubic octamer: on the average, one TMA per *face* of the octamer. At low TMA:SiO_2 ratios, we found that the TMA cations were very mobile, and that their average coordination was one cation per *cube*. We suggested then that the adsorbed TMA molecules must be forming some sort of a protective "shield" around the octamer against hydrolysis of the siloxane bonds (Si−O−Si). Upon TMA adsorption, water molecules, possibly hydrogen bonded to the bridge oxygens, are expelled from the surface of the octamer. By calculating the water oxygen−silicate terminal oxygen pair correlation function, we concluded that, despite the presence of TMA at the surface of Q_8^3, the hydrogen bond network between the water molecules and the terminal surface oxygens (Si−O$^-$) remained intact. In this respect, the average coordination number of water molecules in the vicinity of the terminal oxygens is the same as one would calculate in TMA-free, aqueous solution.

Our interest in these model systems is twofold. First motivation is that, in aqueous solutions and in the presence of TAAs, cage-like species such as the octamer, Q_8^3, or the prismatic

† University of Delaware.
‡ University of Minnesota.

(1) Kinrade, S. D.; Knight, C. T. G.; Pole, D. L.; Syvitski, R. *Inorg. Chem.* **1998**, *37*, 4272−4277.
(2) Kinrade, S. D.; Knight, C. T. G.; Pole, D. L.; Syvitski, R. *Inorg. Chem.* **1998**, *37*, 4278−4283.
(3) Caratzoulas, S.; Vlachos, D.; Tsapatsis, M. *J. Phys. Chem. B* **2005**, *109*, 10429.

 10.1021/ja0561136 CCC: $33.50

hexamer, $Si_6O_{15}^{-6}$ (another species observed by ^{29}Si NMR), form clathrates, as this has been verified by crystallographic methods.[4,5] Silicate clathration, with concomitant TAA occlusion, has been speculated to be the very first step in the formation of precursor species prior to nucleation in zeolite crystal growth.[6−9] For this to happen, SiO_2 units must replace water molecules in the TAA's hydration shell. As they do so, the SiO_2 units start to form small clusters, possibly of cage-like morphology similar to that of the octamer or the hexamer, that can act as precursor species in the nucleation process. A process like this is bound to have an effect on solvent structure and dynamics in the immediate neighborhood of these species, and by that, we primarily imply the hydrogen bond network. Thus, the study of species, such as $Si_8O_{20}^{-8}$ or $Si_6O_{15}^{-6}$, in solution, as well as the analysis of their interactions with TMA or the solvent, will afford us a first glimpse into the mechanism of zeolite formation. We should note that TMA has recently been used as a structure directing agent in the synthesis of a new layered silicate, ERS-12.[10]

The second motivating factor has to do with the remarkable fact that, despite their subnanoscale dimensions, these model, cage-like species already manifest clear signs of control over speciation; TMA stabilizes the octamer in solution, but not the hexamer, which requires a good deal of coercion and the presence of $(CH_3CH_2)_4N^+$ (TEA) and TMA in equal amounts and the presence of a cosolvent (usually methanol).[1,2,11−14] Elucidation of the reasons underlying this preferential stabilization may provide invaluable information on the formation and stabilization of silica nanoparticles. It is well-established that, under hydrothermal conditions, the synthesis of several zeolite types (Si-MFI (silicalite-1), Si-MTW, Si-BEA, and LTA) proceeds through a long-lived metastable state which involves the formation of small colloidal particles, 10 nm or less in diameter.[15−24] A major step in answering a host of questions in zeolite crystallization would be to understand the structure and stabilization of these nanoparticles and the mechanism by which they contribute to the growth of larger crystallites. Central, in all of these questions, is the role of the organic cations. Very little consensus exists regarding these issues. Controversy arises primarily because the analytical techniques that are used (NMR, neutron scattering, X-ray scattering) are either not sensitive to the detailed microscopic structure of these species or else require a considerable degree of interpretation to obtain structural information. The relatively small size of model polyions, such as $Si_8O_{20}^{-8}$ or $Si_6O_{15}^{-6}$, makes them amenable to computer simulation by means of which we can study the interactions between the silicate species and the organic cation on an atomic scale, while taking into account the full effects of the solvent explicitly.

The purpose of this article is twofold. (i) To further examine the validity of the notion of the protective "shield".[1−3,25,26] To that end, we study the prismatic $Si_6O_{15}^{-6}$ (also referred to as "double three-ring" or Q_6^3) in aqueous TMA solution. By carrying out molecular dynamics simulations, we investigate the system in equilibrium and conclude that TMA fails to coordinate around the hexamer even at high TMA:SiO_2 ratios, in stark contrast with our previous findings for the octamer.[3] As mentioned earlier, ^{29}Si NMR experiments have shown that in the presence of TMA the hexamer is always pitted against the octamer.[1,2] Thus, our findings, in conjunction with the NMR conclusions, put the correlation between stability of the polysilicates and TMA ability to adsorb at their surfaces on firmer footing. Furthermore, they reinforce the notion of the protective shield. (ii) To investigate the underlying reasons for which TMA does a better job at stabilizing the octamer than the hexamer. In this respect, first we examine the energetics of this preferential stabilization, and second, we analyze the water structure and dynamics in the vicinity of the silicate solutes and of their complexes with TMA.

Details on the force field and the molecular dynamics simulations are given in the Methods section. Results on the equilibrium studies of the prismatic hexamer in TMA aqueous solution are presented in Results and Discussion sections 3.A.1. and 3.A.2. The energetics of the preferential stabilization of the octamer versus the hexamer are discussed in section 3.B. Solvent structure (hydrogen bond network) and dynamics as they relate to the preferential stabilization are discussed in section 3.C. and 3.D. We conclude in section 4.

2. Methods

A. Simulation. The force field for intermolecular interactions was based on pairwise additive potentials between atomic sites:

$$u_{\alpha\beta}(r) = \frac{q_\alpha q_\beta}{r} + 4\epsilon_{\alpha\beta}\left[\left(\frac{\sigma_{\alpha\beta}}{r}\right)^6 - \left(\frac{\sigma_{\alpha\beta}}{r}\right)^{12}\right] \qquad (1)$$

where α and β denote a pair of interacting sites on different molecules; r is the separation between two interacting sites; q_α is the point charge at site α, and $\epsilon_{\alpha\beta}$ and $\sigma_{\alpha\beta}$ are, respectively, the energy and distance parameters in the Lennard-Jones potential.

For water, we have used the TIPS3P model of Jorgensen.[27] For the silica hexamer and TMA, the Lennard-Jones parameters we used in

(4) Wiebcke, M.; Grube, M.; Koller, H.; Engelhardt, G.; Felsche, J. *Microporous Mater.* **1993**, *2*, 55−63.
(5) Wiebcke, M.; Emmer, J.; Felsche, J. *Microporous Mater.* **1995**, *4*, 149−1587.
(6) Chang, C. D.; Bell, A. T. *Catal. Lett.* **1991**, *8*, 305−316.
(7) Burkett, S. L.; Davis, M. E. *J. Phys. Chem.* **1994**, *98*, 4647−4653.
(8) Burkett, S. L.; Davis, M. E. *Chem. Mater.* **1995**, *7*, 920−928.
(9) Burkett, S. L.; Davis, M. E. *Chem. Mater.* **1995**, *7*, 1453−1463.
(10) Millini, R.; Carluccio, L.; Carati, A.; Bellussi, G.; Perego, C.; Cruciani, G.; Zanardi, S. *Microporous Mesoporous Mater.* **2004**, *74*, 59−71.
(11) Harris, R. K.; Knight, C. T. G. *J. Chem. Soc., Faraday Trans. 2* **1983**, *79*, 1525.
(12) Harris, R. K.; Knight, C. T. G. *J. Chem. Soc., Faraday Trans. 2* **1983**, *79*, 1539.
(13) Knight, C. T. G.; Kirkpatrick, R. J.; Oldfield, E. J. *J. Am. Chem. Soc.* **1986**, *108*, 30.
(14) Knight, C. T. G.; Kirkpatrick, R. J.; Oldfield, E. J. *J. Am. Chem. Soc.* **1987**, *109*, 1632.
(15) Schoeman, B. J.; Sterte, J.; Otterstedt, J. E. *Zeolites* **1994**, *14*, 110−116.
(16) Schoeman, B. J. *Microporous Mesoporous Mater.* **1998**, *22*, 9−22.
(17) Schoeman, B. J.; Higberg, K.; Sterte, J. *Nanostruct. Mater.* **1999**, *12*, 49−54.
(18) Kirschhock, C. E. A.; Ravishankar, R.; Jacobs, P. A.; Martens, J. A. *J. Phys. Chem. B* **1999**, *103*, 11021−11027.
(19) Kirschhock, C. E. A.; Ravishankar, R.; Verspeurt, F.; Grobet, P. J.; Jacobs, P. A.; Martens, J. A. *J. Phys. Chem. B* **1999**, *103*, 4965−4971.
(20) Mintova, S.; Olson, N. H.; Valtchev, V.; Bein, T. *Science* **1999**, *283*, 958−960.
(21) Ravishankar, R.; Kirschhock, C. E. A.; Knops-Gerrits, P. P.; Feijen, E. J. P.; Grobet, P. J.; Vanoppen, P.; Schryver, F. C. D.; Miehe, G.; Fuess, H.; Schoeman, B. J.; Jacobs, P. A.; Martens, J. A. *J. Phys. Chem. B* **1999**, *103*, 4960−4964.
(22) Nikolakis, V.; Kokkoli, E.; Tirrell, M.; Tsapatsis, M.; Vlachos, D. *Chem. Mater.* **2000**, *12*, 845−853.
(23) de Moor, P. P. E. A.; Beelen, T. P. M.; van Santen, R. A.; Beck, L. W.; Davis, M. E. *J. Phys. Chem. B* **2000**, *104*, 7600−7611.
(24) Kragten, D.; Fedeyko, J.; Sawant, K.; Rimer, J.; Vlachos, D.; Lobo, R.; Tsapatsis, M. *J. Phys. Chem. B* **2003**, *107*, 10006−10016.
(25) Harris, R. K.; Jones, J.; Knight, C. T. G.; Newman, R. H. *J. Mol. Liquids* **1984**, *29*, 63−74.
(26) Fedeyko, J. M.; Rimer, J. D.; Lobo, R. F.; Vlachos, D. G. *J. Phys. Chem. B* **2004**, *108*, 12271−12275.
(27) Jorgensen, W. L. *J. Chem. Phys.* **1982**, *77*, 4156.

Table 1. Intermolecular Potential Parameters

atom	ϵ (kcal/mol)	σ (Å)	q
	water[a]		
O	0.1521	3.1501	−0.834
H	0.0	0.0	0.417
	tetramethylammonium (TMA)[b]		
N	0.17	3.25	0.289
C	0.12	3.29	−0.302
H	0.02	1.78	0.160
	silica hexamer ($Si_6O_{15}^{6-}$)[b]		
Si	0.04	4.053	1.77
O_b[c]	0.105	3.35	−1.04
O_t[c]	0.105	3.35	−1.22

[a] TIPS3P, ref 27. [b] Partial charges, this work; Lennard-Jones parameters from CFF93. [c] O_b siloxane, bridge oxygen; O_t silanol, terminal oxygen

this study are given in Table 1. For cross-species interactions, the relevant Lennard-Jones parameters were obtained by the Lorentz−Berthelot rules.[28]

All partial charges have been obtained by ab initio calculations, at the same theory level for all solute molecules; specifically, Hartree−Fock with the 6-31G(d) basis set, while the Self-Consistent Isodensity Polarizable Continuum Model (SCIPCM)[29] was employed to take the water solvent into account. The partial charges were subsequently obtained using the CHELPG[30] scheme as implemented in Gaussian. In the CHELPG (CHarges from ELectrostatic Potentials using a Grid based method) scheme, atomic charges are fitted to reproduce the molecular electrostatic potential at a number of points around the molecule. CHELPG charges are superior to Mulliken charges as they depend much less on the underlying theoretical method used to compute the wave function (and thus the molecular electrostatic potential surface). The partial charges for all the molecules are given in Table 1.

All types of molecules in our simulations were held rigid. Specifically, for both the hexamer and the TMA molecules, we adopted configurations which had previously been optimized in vacuo by ab initio methods. For the geometry of the water molecules, we have taken the bond lengths equal to 0.9573 Å and the bond angle equal to 104.52°.

The equilibrium studies of the hexamer in aqueous TMA solution were performed by simulating the mixture at the following concentration: 1 $Si_6O_{15}^{6-}$:12 TMA:365 H_2O, which corresponds to the maximum silica to TMA ratio that was used by Kinrade et al.[1] in their NMR experiments (namely, 1.0 mol/kg SiO_2:2.0 mol/kg TMA.) The simulation box also contained 6 OH^- ions for electroneutrality. To obtain a starting configuration, one hexamer along with 12 TMA molecules and 6 hydroxyl ions was optimized in vacuo. The whole "assembly" was subsequently placed in a water cavity at the center of a cubic simulation box of lattice constant 22.173 Å. The system was then optimized to remove accidental overlaps between interaction sites. The simulation extended up to 2.0 ns, of which the first 500 ps were the equilibration period.

To have a reference for the solvent structure in the vicinity of the silicate polyion, the simulation was repeated for TMA-free solution at the same water density. For this system, the molecular dynamics trajectories were extended up to 500 ps, of which the initial 250 ps were equilibration.

We performed the MD simulations using periodic boundary conditions in the NVT ensemble (constant temperature, volume, and number of particles) at $T = 300$ K with Nosé-Hoover thermostat. The equations of motion were integrated using the Verlet algorithm, and bond constraints for the rigid molecules were enforced using the SHAKE algorithm.[28] A time step of 1 fs was adequate to satisfy energy conservation (for the extended system[31]) in both cases. For the short-range forces, we employed the minimum image convention with a cutoff distance equal to half the simulation box length. For the long-range electrostatic forces, we used Ewald summation.[31]

The DL_POLY parallel molecular dynamics simulation package developed at the Daresbury Laboratory, UK, was used.[32]

B. Methodology for Hydrogen Bond Analysis. A crucial issue in this study is solvent structure (hydrogen bond network) and dynamics. Because we expect water molecules in the immediate vicinity of different functional groups of a solute or in the vicinity of different species of solutes to behave differently, we shall classify them according to their average distance from the various functional groups of the solute(s).[33] By this grouping, we obtain the advantage that we can investigate separately the structural and dynamic properties of solvent molecules which are more strongly influenced by a functional component of a solute molecule than by another. In our case, this sort of classification leads to three groups of water molecules. First, we will have those which on the average spend most of their time in the vicinity of the oxygen atoms of the polysilicate anion—we shall be referring to them as the "polar" water molecules. In the second group, we shall have the water molecules which on the average spend most of their time in the immediate vicinity of the methyl groups of TMA, that is, in its first solvation shell, and we shall be referring to them as the "nonpolar" water molecules. Finally, in the third group, we shall have the "bulk" water molecules. Quantitatively, the classification will be made according to a procedure whereby molecules will be assigned to certain well-defined, spatial or even energy regions.

In general, let $i = 1, 2, ..., N$ be an index that runs through the water molecules, and α_j ($j = 1, 2, ..., M_\alpha$) denote the j-th functional component of type α of a solute molecule, for example, the oxygen atoms of the polysilicate anion, or the carbon atoms of TMA, or even an entire solute species. Let us then define $d_{i\alpha_j}(t)$ to be a norm measuring "distance", in some space, between molecule i of the solvent and the functional group α_j, as a function of time, t, along a trajectory. For example, the space may be the Euclidean space, in which case $d_{i\alpha_j}(t)$ will be the usual Euclidean norm measuring physical distance in configuration space, or an energy space, in which case the $d_{i\alpha_j}(t)$ will be measuring energy differences or pair interaction energies (i.e., location on a potential energy surface), etc. Then, we can compute

$$d_{i\alpha}(t) \equiv \min_{j\in\{1,...,M\alpha\}} d_{i\alpha_j}(t) \tag{2}$$

and from that the time average

$$\bar{d}_{i\alpha} = (1/T)\int_0^T d_{i\alpha}(t)\,dt \tag{3}$$

Thus, from all the M_α functional groups of a certain type α, eq 2 picks out the one that is the closest to the water molecule i at time t and records the "distance". Then, by eq 3, that is by time averaging, we compute the mean distance of molecule i to the functional components of type α. If $\bar{d}_{i\alpha} \leq d_{c\alpha}$, where $d_{c\alpha}$ is some cutoff defining the group, then the i-th water molecule will be "assigned" to the group which is associated with the functional component α.

In this study, for the polar and nonpolar classes, we choose the cutoff values $d_{cp} = 4.0$ Å and $d_{cn} = 5.0$ Å, respectively. Specifically, a polar molecule i will be one for which $\bar{d}_{ip} \leq d_{cp}$, where $\bar{d}_{ip}$ is its average distance from the silicate oxygens. If for the mean distance, $\bar{d}_{in}$, of the water molecule from TMA carbon atoms we have $\bar{d}_{in} \leq d_{cn}$, but $\bar{d}_{ip} > d_{cp}$ (i.e., it is not polar), then the water molecule will be assigned to the nonpolar group. The bulk water molecules will be all the rest.

A solvent molecule in a certain group does not spend its entire life within the spatial region associated with that group. Rather, in the course

(28) Allen, M. P.; Tildesley, D. J. *Computer Simulation of Liquids;* Clarendon: Oxford, 1987.
(29) Foresman, J. B.; Keith, T. A.; Wiberg, K. B.; Snoonian, J.; Frisch, M. J. *J. Phys. Chem.* **1996**, *100*, 16098−16104.
(30) Breneman, C. M.; Wiberg, K. B. *J. Comput. Chem.* **1990**, *11*, 361−373.
(31) Frenkel, D.; Smit, B. *Understanding Molecular Simulation;* Academic Press: New York, 2001.
(32) Smith, W.; Forester, T. *J. Mol. Graphics* **1996**, *14*, 136.
(33) Rossky, P. J.; Karplus, M. *J. Am. Chem. Soc.* **1979**, *101*, 1913−1937.

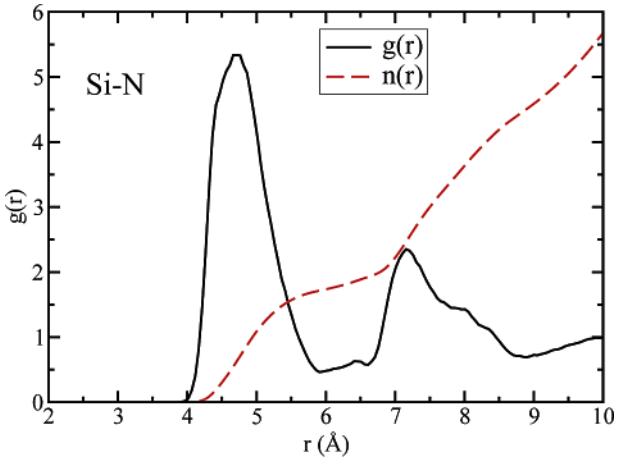

Figure 1. Hexamer silica−TMA nitrogen pair correlation function, $g(r)$, (black, solid line) and corresponding running coordination number, $n(r)$ (red, dashed line).

of a simulation, and depending on its mean square displacement and location relative to the region's dividing surface, the molecule may get in and out of that region and thus change identity quite a few times. That notwithstanding, since the classification is made on the basis of the time-averaged norm $\bar{d}_{i\alpha}$, it is reasonable to expect that certain ensemble-averaged properties of the molecule will be influenced by the fact that most of the time the molecule i is in the immediate vicinity of the functional groups α. If such influences are indeed identified, then we will also have a physical justification for the decomposition of the solvent into groups.

In anticipation of the analysis we undertake in section 3.C, we should note, in passing for the moment, that the suggested solvent classification is meaningful and from an energetic point of view, and that solvent classification could be made on the basis of energy criteria instead of spatial ones.

3. Results and Discussion

A. Structure. 1. Hexamer−TMA Complex. The optimized geometry of the hexamer is that of a regular, right triangular prism. We study the structure of the putative hexamer−TMA complex in solution by looking at the various atom−atom pair correlation functions, $g_{\alpha\beta}(r)$, and corresponding running coordination numbers

$$n_{\alpha\beta}(r) = 4\pi\rho_\beta \int_0^r g_{\alpha\beta}(r')\, r'^2\, dr' \qquad (4)$$

where ρ_β is the bulk number density of atom β.

The first object of our interest is the Si−TMA nitrogen pair correlation function, $g_{SiN}(r)$ (solid, black line in Figure 1). There is a high peak at 4.7 Å and a second, much broader, low peak at 7.0 Å. The two distinct peaks imply that the TMA molecules coordinate opposite the faces of the hexamer. It is a simple matter to obtain details about the coordination geometry. Let a, b be the Si−Si separation in the three-ring and four-ring face of the prism, respectively. From the in vacuo optimized geometry, we have $a = 3.06$ and $b = 3.2$ Å (cf. Figure 2). Assuming that the TMA nitrogen lies in a C_2 symmetry axis of the hexamer and a distance r_{4R} from the four-ring face ($4R$), we expect a peak at $p_{4R} = (1/2)(a^2 + b^2 + 4r_{4R}^2)^{1/2}$ and a second peak at $p'_{4R} = (1/2)[(2\, r_{4R} + a\sqrt{3})^2 + b^2]^{1/2}$. For $p_{4R} = 4.7$ Å, we obtain $p'_{4R} = 6.98$ Å, in agreement with the location of the second peak in $g_{SiN}(r)$ in Figure 1. Similarly, assuming that the TMA nitrogen lies in the C_3 symmetry axis and a distance r_{3R} from the three-ring face ($3R$), we expect a peak at $p_{3R} = (r_{3R}^2 + a^2/3)^{1/2}$ and a second peak at $p'_{3R} = [(r_{3R} + b)^2 + a^2/3]^{1/2}$. For $p_{3R} = 4.7$ Å, we obtain $p'_{3R} = 7.8$ Å; note the shoulder at 7.9 Å in the second peak of $g_{SiN}(r)$. Therefore, the TMA molecules prefer to be opposite $4R$ faces rather than $3R$ faces; the latter remain exposed to the water environment. Upon integration of $g_{SiN}(r)$ [cf. eq 4], we find that 1.7 nitrogen atoms are on the average within a radius of 6.0 Å of a Si atom (red, dashed line in Figure 1). So, on the average, 2.8 TMAs adsorb onto the surface of the hexamer. This number is consistent with the earlier conclusion that the TMAs prefer to coordinate opposite the four-ring faces, of which there are three in the prismatic hexamer; a typical configuration along the molecular dynamics trajectory is shown in Figure 3.

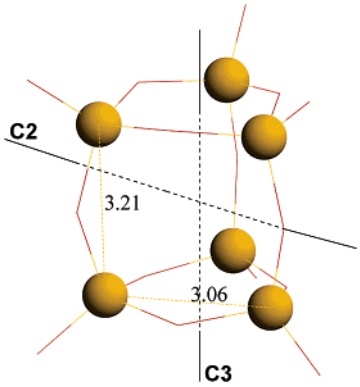

Figure 2. Hexamer geometry.

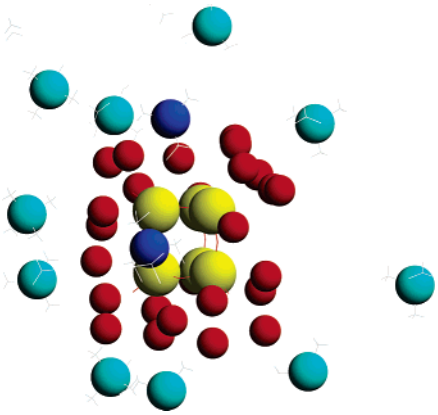

Figure 3. Representative configuration in the vicinity of the silica hexamer. Color coding: Si atoms, yellow balls; water oxygen, red balls; TMA nitrogen atoms within a radius of 6.5 Å of Si atoms, blue balls; rest of TMA nitrogen atoms, cyan balls. (Radii not drawn to scale.)

Thus, at equilibrium, the organic cations fail to cover fully the surface of the hexamer. This is in stark contrast with our findings for the cubic octamer; at such high TMA:SiO_2 ratios, we have found that six TMA molecules coordinate around it.[3]

2. Solvent. Next, we investigate the solvent structure around the silicate solute. In Figure 4, we show the Si−water oxygen pair correlation function, $g_{SiO_W}(r)$ (black, solid line), and we compare it with that obtained from the simulation without TMA (red, dashed line). The differences between them are due to the partial TMA adsorption and the resulting water expulsion from the surface. For comparison, we also have plotted the $g_{SiO_W}(r)$ (green, dash−dotted line) obtained from the simulation of the $Si_8O_{20}^{-8}$−TMA−H_2O mixture at the same TMA:SiO_2 ratio.[3] Because all six faces of the octamer are "occupied" by TMA,

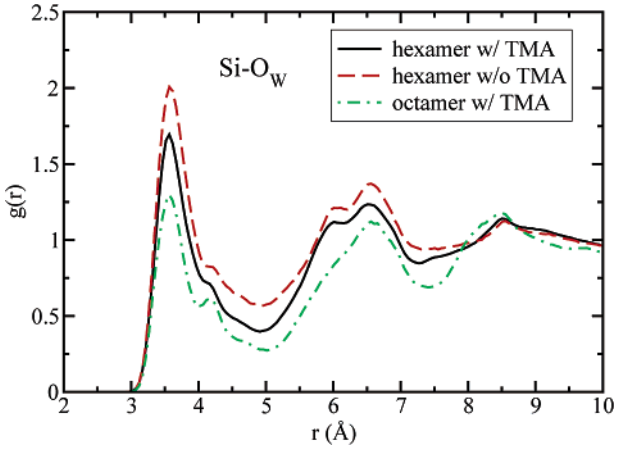

Figure 4. Silica−water oxygen pair correlation function. The solid, black line is for the $Si_6O_{15}^{-6}$−TMA−H_2O mixture for concentration of 2.0 mol/kg TMA:1.0 mol/kg SiO_2. The red, dashed line is for the $Si_6O_{15}^{-6}$−H_2O mixture, that is, in the absence of TMA. For the sake of comparison, we have included the $g_{SiO_w}(r)$ for the $Si_8O_{20}^{-8}$−TMA−H_2O mixture at the same TMA:SiO_2 ratio (green, dash−dotted line).

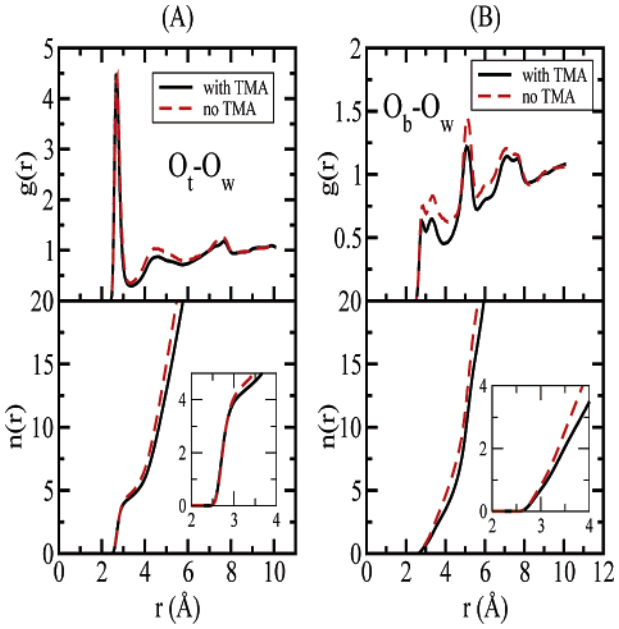

Figure 5. Left panels (A): In the upper panel, we show the hexamer terminal oxygen−water oxygen pair correlation function, $g_{O_tO_w}(r)$, for the hexamer−TMA−water mixture (black, solid line) and for TMA-free solution (red, dashed line). The corresponding running coordination numbers, $n_{O_tO_w}(r)$, are given in the lower panel. The inset shows $n_{O_tO_w}(r)$ in the range 2−4 Å. Right panels (B): Same as in (A), but for the bridge oxygen−water oxygen pair; $g_{O_bO_w}(r)$ in the upper panel and corresponding $n_{O_bO_w}(r)$ in the lower panel. The $g_{O_tO_w}(r)$ for the hexamer−TMA−water solution is the same as for TMA-free solution. Minor differences exist between the $g_{O_bO_w}(r)$ due to partial TMA adsorption onto the surface of the hexamer.

the peak at 3.5 Å is significantly lower than that in the partially covered hexamer.

A very interesting picture of the solvent structure is provided in Figure 5. In the left panels (A), we show the hexamer terminal oxygen−water oxygen pair correlation function, $g_{O_tO_W}(r)$, and corresponding running coordination numbers, $n_{O_tO_W}(r)$, for two solution mixtures: one with TMA and the second without. In the right panels (B), we show the same information but for the hexamer bridge oxygen−water oxygen pair correlation function, $g_{O_bO_W}(r)$. In both solution mixtures, the first peak in $g_{O_tO_W}(r)$

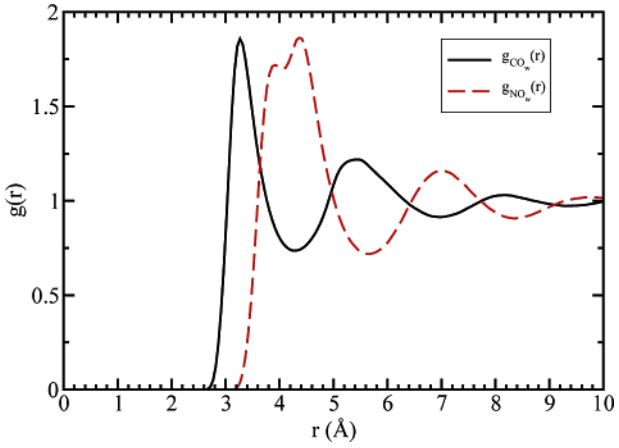

Figure 6. Water structure around the TMA molecules as revealed by the carbon−water oxygen, $g_{CO_w}(r)$, and nitrogen−water oxygen, $g_{NO_w}(r)$, pair correlation functions.

occurs at approximately the *optimum hydrogen bond distance* of 2.7 Å, and it corresponds very closely to $g_{O_WO_W}(r)$ for pure TIPS3P water.[27] Thus, although some water molecules leave the surface of the hexamer as a consequence of partial TMA adsorption, the hydrogen bond network between the terminal oxygens of the surface and the water molecules remains *intact*. Upon integration of $g_{O_tO_W}(r)$, we find that three water molecules are on the average within 2.7 Å of each terminal oxygen of the surface. This is consistent with data from X-ray crystallography by Wiebcke et al.[4,5]

The water structure around the TMA solute is typical of that of water around small hydrophobic molecules, despite its net positive charge. In Figure 6, we show the TMA carbon−water oxygen pair correlation function, $g_{CO_W}(r)$ (black, solid line). The increased density in the vicinity of the solute is due to the tendency of water to retain its hydrogen bond network.

Despite their different geometries, there is remarkable similarity between the two polyions, Q_8^3 and Q_6^3, in aqueous environments, in the sense that both participate in strong hydrogen bonds with the solvent, with or without TMA in the solution mixture. However, Q_6^3 cannot support a TMA layer around it, and there ought to be a correlation between this and the fact that Q_6^3 is not as stable a species as Q_8^3.

We mentioned earlier that the NMR data show that, at high TMA:SiO_2 ratios, Q_6^3 is always pitted against Q_8^3. In fact, it is the Q_6^3 NMR peak that one observes in the beginning before it disappears over time in favor of Q_8^3.[1] Therefore, it appears as though Q_6^3, rather its complex with TMA, is a long-lived metastable species. Thus, it is of interest to examine the energetics of this preferential stabilization and see whether the Q_6^3−TMA complex could indeed be a metastable state of the system.

B. Energetics−Hexamer versus Octamer. A measure of the thermodynamic driving force for this preferential stabilization is the relative change in the free energies of formation of the corresponding polysilicate−TMA complexes:

$$\Delta\Delta F_f^{(l)} = \Delta F_f^{(l)}(Q_8^3 \cdot n\mathrm{TMA}) - \Delta F_f^{(l)}(Q_6^3 \cdot m\mathrm{TMA}) \quad (5)$$

where $\Delta F_f^{(l)}$ denotes free energy of formation in liquid phase. By making use of thermodynamic cycles and suppressing bond energetics, the formation free energy change in liquid phase can be expressed in terms of the gas phase formation energy

and the solvation free energies of the participating molecular species:

$$\Delta F_f^{(l)}(Q^3{}_n\cdot n'\mathrm{TMA}) = \Delta E^{(g)}{}_f(Q_n{}^3\cdot n'\mathrm{TMA}) + \Delta F_{sol}(Q_n{}^3\cdot n'\mathrm{TMA}) - \Delta F_{sol}(Q_n{}^3) - n'\Delta F_{sol}(\mathrm{TMA}) \quad (6)$$

where ΔF_{sol} denotes solvation free energy, and $\Delta E_f^{(g)}$ is the gas phase formation energy.

In the following, we investigate the relative stability between the *neutral* complexes ($n = 8$, $m = 6$ in eq 5) for two reasons. First, on the formation of $Q_8{}^3$, in ref 1, Kinrade et al. proposed the reaction equilibria

$$8\ H_3SiO_4^- + x\mathrm{TMA}^+ \rightleftarrows [Si_8O_{20} \times x\mathrm{TMA}]^{(8-x)-} + 12\ H_2O$$

For $[OH^-]:[Si] \geq 1$, analysis of their NMR data gave $x = 8 \pm 1$. This is in accordance with charge balance considerations and does not contradict our findings in ref 3, namely, that the TMA layer around $Q_8{}^3$ consists of six TMAs. Thus, it is reasonable to consider the stability of the neutral complex $Q_8{}^3\cdot 8$TMA and, to treat $Q_8{}^3$ and $Q_6{}^3$ on equal footing, one should also consider the neutral complex $Q_6{}^3\cdot 6$TMA. The second reason is to avoid ambiguities stemming from differences in excess charge. For example, if in eq 5 we took $n = 6$ and $m = 5$, then the corresponding complexes would carry net charge of -2 and -1. In such a case, the difference in solvation energies $\Delta F_{sol}(Q_8{}^3\cdot n\mathrm{TMA}) - \Delta F_{sol}(Q_6{}^3\cdot m\mathrm{TMA})$ would mostly reflect the difference in the excess charges ($O(q^2)$, where q denotes excess charge), since $Q_8{}^3$ and $Q_6{}^3$ create approximately the same solvent cavity (with a radius of $\sim$5.0 Å according to reaction field ab initio calculations).

To compute the solvation energies, while using explicit solvent free energy perturbation or thermodynamic integration methods provide a solution to the problem, such calculations require a major computational effort if converged results are required, especially for the silicate−TMA complexes. Here, we obtain estimates for the solvation energies using the Generalized Born (GB) solvation model, whereby the solvent is treated as a statistical continuum.[34] For a solute with n atoms, GB creates a cavity of radius a_i around the i-th atom, with the partial charge q_i of the atom at the center of the dielectric cavity. Then the polarization term of the solvation free energy is given by the formula

$$\Delta F_{sol} = -\frac{1}{2}\left(1 - \frac{1}{\epsilon}\right)\sum_{i=1}^{n}\sum_{j=1}^{n}\frac{q_i q_j}{f_{GB}} \quad (7)$$

where $f_{GB} = (r_{ij}{}^2 + a_{ij}{}^2\, e^{-D})^{1/2}$, $D = [r_{ij}/(2a_{ij})]^2$, and $a_{ij} = (a_i a_j)^{1/2}$; $\epsilon = 78.39$ models the aqueous environment. We set an atomic cavity radius, a_i, equal to the sum of the van der Waals radius ($\sigma/2$) of the atom (Table 1) and that of the solvent radius. The GB model has been extensively used to model solvation effects in small and large biomolecular systems. Typically, the water molecule radius is taken between 1.3 and 1.5 Å;[35] here we set it equal to 1.5 Å, to be consistent with the oxygen van der Waals radius in TIPS3P water.

Table 2. Solvation Free Energies Obtained from the Generalized Born Model, Equation 6, and Gas Phase Energies of Formation[a]

	TMA	$Q_8{}^3$	$Q_6{}^3$	$Q_8{}^3\cdot 8$TMA	$Q_8{}^3\cdot 8$TMA
$\Delta E_f^{(g)}$				−2311	−1449
ΔF_{sol}	−50.8[b]	−1846.7	−1132.0	−142.8	−117.9
$\Delta F_f^{(l)}$				−200.7	−130.1
				$\Delta\,\Delta F_f^{(l)} = -70.6$	

[a] The liquid phase formation free energies for the silicate−TMA complexes are obtained using eq 6 (energies in kcal/mol.) [b] Experimental value = −51 ± 0.5 kcal/mol.

For each $Q^3{}_n\cdot n$TMA complex, the gas phase energy of formation, $\Delta E_f^{(g)}(Q^3{}_n\cdot n\mathrm{TMA})$, is reported relative to the state in which all molecular species are at infinite separation; they were computed by energy minimization.

The calculated energies are summarized in Table 2. For TMA, the calculated value of −50.8 kcal/mol is in very good agreement with the experimental value of −51 kcal/mol.[36] We are not aware of any experimental values for the solvation free energies of the other species, of $Q_8{}^3$ and $Q_6{}^3$ in particular, so comparison with experimental data is not possible at the present time. That notwithstanding, our confidence on these estimates should primarily rely on the following two facts: (i) for charged solute molecules, the solvation free energy is primarily determined by electrostatics and thus solvent polarization; and (ii) the partial charges have been obtained by electronic structure calculations, as discussed in section 2.

Then, by eqs 5 and 6, we find that both complexes are stable ($\Delta F_f^{(l)} < 0$), but there is a thermodynamic driving force $\Delta\Delta F_f^{(l)} \approx -70$ kcal/mol in favor of the $Q^3{}_8\cdot 8$TMA complex. This result would thus be consistent with the notion that the hexamer−TMA complex is a metastable state, evidently favored by kinetics. Eventually, however, TMA desorbs off the surface of the hexamer, leaving it vulnerable to hydrolysis.

The inability of TMA to remain at the surface of the hexamer cannot be explained without taking account of the solvent. We have run numerous molecular dynamics trajectories with different initial conditions for the hexamer−TMA complex, at various concentration conditions. All initial conditions involved "preformed" complexes, which were subsequently immersed in water. In all the cases, the solvent molecules were able to expel the cations from the surface. Studying the dynamical behavior of the system we used for the structural studies of the previous section (1 $Si_6O_{15}{}^{6-}$:12 TMA:365 H_2O), we observe that in the beginning TMA desorption appears to occur in a rather smooth, continuous fashion, with the distal TMAs peeling off earlier than those proximate to the hexamer. During this phase of the dynamics, water molecules slowly reorganize and creep up onto the surface of the hexamer. As soon as wetting of a face of the hexamer has occurred, the TMA molecule previously coordinated opposite that face desorbs. Interestingly, once a TMA molecule has suffered this fate, the rest follow rather quickly and undergo thereafter a diffusive motion, which may or may not include sojourns back onto the surface. One such trajectory is shown in Figure 7 for the 1 $Si_6O_{15}{}^{6-}$:12 TMA:365 H_2O system, where we plot the hexamer separation from each of the 12 TMA molecules. This MD trajectory corresponds to dry

(34) Still, W.; Tempczyk, A.; Hawley, R.; Hendrickson, T. *J. Am. Chem. Soc.* **1990**, *112*, 6127−6129.
(35) Ooi, T.; Oobatake, M.; Nemethy, G.; Scheraga, H. *Proc. Natl. Acad. Sci. U.S.A.* **1987**, *84*, 3086−3090.
(36) Luzhkov, V. B.; Österberg, F.; Acharya, P.; Chattopadhyaya, J.; Aqvist, J. *Phys. Chem. Chem. Phys.* **2002**, *4*, 4640−4647.

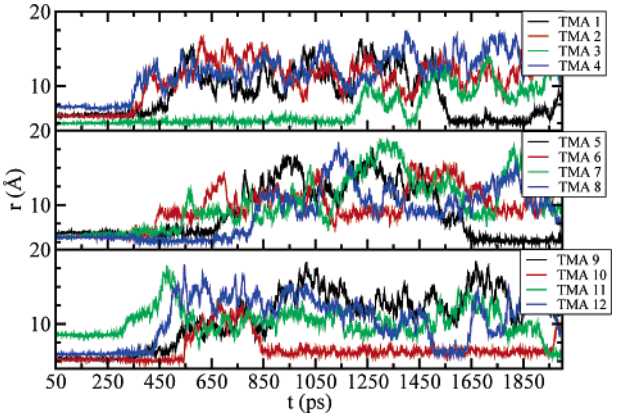

Figure 7. TMA−hexamer separation as a function of time. Data obtained from molecular dynamics trajectory with dry initial conditions and include equilibration period.

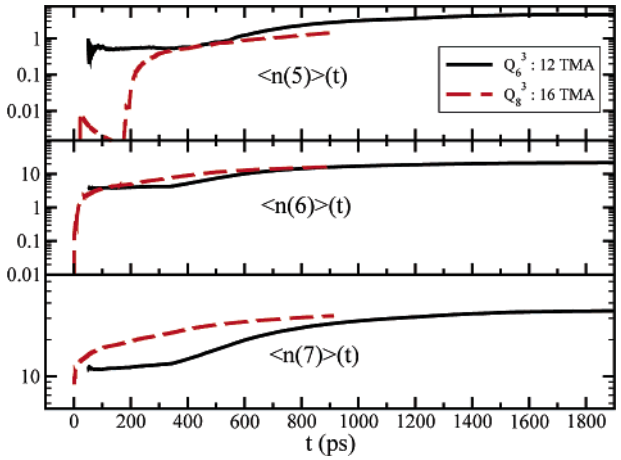

Figure 8. Average number, $\langle n(r)\rangle(t)$, of water molecules within a radius r from the silicate center of mass, as a function of time. Black line refers to the hexamer; red dotted line refers to the octamer ($\langle n(r)\rangle(t)$ drawn on logarithmic scale.)

initial conditions, namely, the complex was prepared in vacuo with TMAs fully coordinated around the hexamer and subsequently immersed in a solvent cavity with no water molecules inside the sphere that defines the second TMA layer. Apart from solvent reorganization, nothing else really happens for about 300 ps, at which moment $(TMA)_{11}$, located ~8.5 Å from the center of the hexamer, leaves the pack. $(TMA)_2$ and $(TMA)_4$ follow 50 ps later, and by $t = 600$ ps, only 2 TMAs linger at the surface. By this time, the hydrogen bond network between the hexamer and the solvent is fully established. Of the cations initially attached to the surface of the hexamer, only $(TMA)_3$ is still there at $t \approx 1250$ ps.

We can follow what the solvent does in the course of this trajectory by monitoring, in time, the average number, $\langle n(r)\rangle(t)$, of water molecules within a radius r from the center of the hexamer. The black lines in Figure 8 show $\langle n(r)\rangle(t)$ for $r = 7$, 6, and 5 Å. Notice the two different temporal regimes. We observe the initially very slow, almost exponential, growth of $\langle n(r)\rangle(t)$. This represents the reorganization phase, whereby water molecules slowly find their way toward the surface of the hexamer. Then, at 340, 350, and 440 ps, respectively, we see the onset of the second regime, which is characterized by faster and nonexponential $\langle n(r)\rangle(t)$ growth. The initial creeping water motion appears to be the rate-determining step in the "dissociation" of the hexamer−TMA complex and possibly in the hydrolysis of the hexamer, although a definitive answer for the latter would require more information regarding the hydrolysis reaction itself. That notwithstanding, it would appear that the relatively long time that it takes for the wetting of the surface of the hexamer to occur, and for TMA to desorb, is consistent with the notion that under these conditions the hexamer is a rather long-lived, metastable species; for some reason we cannot currently explain, this species appears also to be kinetically favored.

The red lines in Figure 8 show $\langle n(r)\rangle(t)$ from an analogous simulation (i.e., dry initial conditions) for the octamer system 1 $Si_8O_{20}^{8-}$:16 TMA:450 H_2O; in this system, at equilibrium, the octamer supports a TMA layer consisting of six cations. Here, the solvent reorganization takes no more than 50 ps. Within this time, the hydrogen bond network between the octamer and the water molecules is established, and the outer TMA layers around it begin to desolve.

C. Hydrogen Bond Network. It is becoming increasingly obvious that the solvent dynamics plays a very important role in the stabilization of these species. It is thus of interest to study the solvent structure in more detail and, in particular, the hydrogen bond network. By acknowledging that the structural and dynamic properties of water are strongly influenced by the functional groups in its vicinity,[33] we have decided to classify water molecules according to their average distance from the various functional groups of the solute(s), as detailed in section 2.A.2. Three water groups result: polar, which on the average spend most of their time in the vicinity of silicate oxygens; nonpolar, which spend most of their time around the TMA methyl groups; and bulk. We remind the reader that, for the polar and nonpolar classes, we have chosen the cutoff values $d_{cp} = 4.0$ Å and $d_{cn} = 5.0$ Å, respectively. The former is the first local minimum in $g_{O_tO_w}(r)$ (cf. Figure 5); the latter has been motivated by the pair distribution function $g_{CO_w}(r)$ (cf. Figure 6).

What we wish to examine is the hydrogen bond network in the vicinity of the solutes and relate potential changes in solvent structure or dynamics to various degrees of TMA coordination around the silicate polyions. To that end, we shall investigate the hydrogen bond network of the water molecules in the following systems:

S1: 1 $Si_8O_{20}^{8-}$:670 H_2O; to establish a reference for the octamer.

S2: 1 $Si_8O_{20}^{8-}$:8 TMA:670 H_2O; with the TMA molecules *constrained* at the surface of the octamer in a geometry determined by in vacuo energy minimization. In essence, in this system, the solute is the complex $Si_8O_{20}^{8-}$·8TMA, with the implied fixed stoichiometry.

S3: 1 $Si_8O_{20}^{8-}$:16 TMA:450 H_2O; same as system C_1 in ref 3, with the TMAs *free* to move. As noted earlier (cf. Methods), this system corresponds to the highest TMA:SiO_2 ratio necessary for Q_8^3 formation and for which our simulations have shown that at equilibrium six TMA molecules coordinate around the octamer.

S4: 1 $Si_6O_{15}^{6-}$:670 H_2O; to establish a reference for the hexamer.

S5: 1 $Si_6O_{15}^{6-}$:6 TMA:670 H_2O; with the TMA molecules *constrained* at the surface of the hexamer in a geometry determined by in vacuo energy minimization. As in S2, in this

Table 3. Number of Water Molecules in Each of the Three Solvent Groups for the Various Systems Considered[a]

system	S1	S2	S3	S4[b]	S5	S6[b]
polar occup.	17	16	27	0 (10)	21	0 (5)
nonpolar occup.		8	208		8	232 (225)
bulk occup.	653	646	215	670 (660)	651	133 (135)

[a] For systems without TMA in solution, there are no entries for the nonpolar class. [b] Number in parentheses is group occupancy based on energetic criterion as explained in the text.

system, the solute is the complex $Si_6O_{15}^{6-}$·6TMA, with the implied fixed stoichiometry.

S6: 1 $Si_6O_{12}^{6-}$:12 TMA:365 H_2O; this is the system used for the structural studies presented in section 3.A., with no constraints imposed on the TMAs. Recall, that in this case at equilibrium the TMA layer consists of only 2.8 molecules.

We shall examine the number of hydrogen bonds formed by a typical water molecule in each of the three solvent groups. For all the systems S1−S6, solvent classification information is collected in Table 3. In all the systems, the time averaging in eq 3 has been performed after full equilibration. One immediate observation we make is that for the S4 and S6 systems the procedure yields zero polar water molecules. Recall that in S4 we have no TMA in the solution, whereas in S6, we do, but they fail to coordinate around the hexamer (cf. section 3.A.). This does not imply, of course, that solvent molecules are not coordinated around the hexamer in S4 or S6. Quite the contrary, as the relevant pair distribution functions reveal. It does, however, suggest that an individual water molecule in the immediate vicinity of a silicate oxygen spends, on the average, very little time in that region of the solution, and that the corresponding water−solute hydrogen bond, if formed at all, is very short-lived. The only hexamer system, of the three considered here, for which our procedure succeeds to yield polar water is the one in which the TMA molecules have been *constrained* to remain at the surface of the hexamer (S5). Placed within the context of the function of TMA in the stabilization of these species, we believe that this is a significant development, and we shall return to it in the next subsection.

In section 2.B., we noted in passing that the suggested solvent classification is meaningful and from an energetic point of view. Indeed, for the species Q_n^3 ($n = 6$ and 8) in water solvent (no TMA), we have calculated the pair interaction energy, ϵ, between each water molecule and the polysilicate anion; the energy ϵ is computed by summing over all interaction sites in the solute for each water molecule, and the distribution is constructed over an entire MD trajectory, 500 ps after equilibration. The distribution density, $n(\epsilon)$, for these pair interaction energies is shown in Figure 9; $n(\epsilon)d\epsilon$ is the average number of water−Q_n^3 pairs with interaction energy between ϵ and $\epsilon + d\epsilon$. There is a dominant peak at $\epsilon \approx 0$ and a low peak at the most negative energies. The contributions to the latter correspond to the water molecules that are hydrogen bonded to the silicate solute. There is a clear local minimum between the two peaks, which could be used as an energy cutoff between the polar (i.e., hydrogen bonded to the solute) and the bulk water molecules. Thus, the solvent classification could be made on the basis of energy criteria instead of spatial ones. The contributions to $n(\epsilon)$ at the highest energies correspond to water molecules which, because of thermal motions in the system, find themselves in close, repulsive contact with the solute atoms and far from the

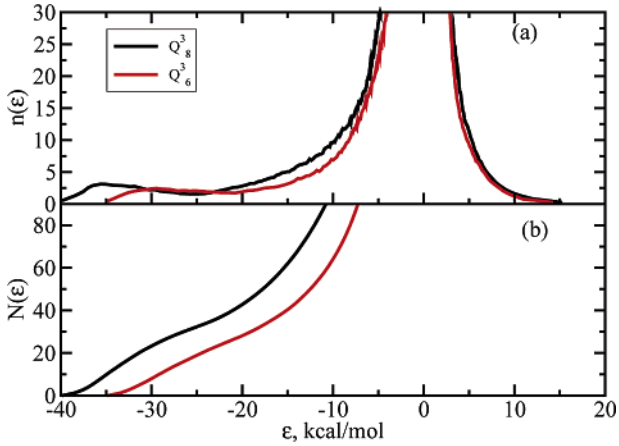

Figure 9. (a) Distribution density of the water−Q_n^3 ($n = 8$ and 6) pair interaction energies, including all water molecules. Black line refers to the octamer, Q_8^3; red line refers to the hexamer, Q_6^3. (b) The cumulative distributions of the densities in (a); $N(\epsilon)$ is the average number of water−silicate pairs with interaction energy less than or equal to ϵ. The distributions are normalized to the total number of water molecules in the simulation box, namely, $N(\infty) = 670$.

potential energy minimum. The dominant peak around zero is of course due to the fact that a large number of molecules are far from the solute, with nearly zero interaction energies.

Thus, to make progress, for the S4 and S6 systems, we divide the solvent molecules into groups by making use of the energetic criterion, rather than the spatial one. From the distribution for water−hexamer pair interactions (shown in Figure 9 for S4), if the time-averaged energy between a water molecule and the hexamer is less than or equal to a cutoff value ϵ_{cp}, then the water molecule will be labeled as polar. We have found that the ϵ_{cp} energy value that yields nonzero polar occupancy is system dependent and, to determine it, one has to analyze the corresponding distribution $n(\epsilon)$ for each system individually. Here, we have set it to the most negative value at which the corresponding $n(\epsilon)$ starts a steep rise toward the dominant peak at $\epsilon \approx 0$. In S4, we have taken $\epsilon_{cp} = -15.0$ kcal/mol (cf. Figure 9); in S6, $\epsilon_{cp} = -10.5$ kcal/mol ($n(\epsilon)$ for S6 is not shown here). We should make a final note regarding this procedure. The energetic and the spatial criteria for water classification are rather equivalent, in the sense that, for example, nonzero occupancy for the polar group in S4 could have been achieved by increasing the spatial cutoff d_{cp} from 4.0 to 5.0 Å; in S6, the d_{cp} increase would have been even larger, from 4.0 to 6.0 Å. However, for either of the these systems, setting the equivalent physical distance cutoff value, without guidance from the distribution for the pair interaction energies, would have been rather arbitrary. The larger d_{cp} values for the S4 and S6 systems imply that the water molecules that contribute to the lowest energies in the distribution $n(\epsilon)$ are not, on the average, in very close proximity to the hexamer.

Self-consistency in the classification procedure required that the energy criterion be used in the definition of the nonpolar group, too. From the analogous distributions for water−TMA pair interaction energies (not shown here), we have set the nonpolar cutoff to $\epsilon_{cn} = -3.5$ kcal/mol; this has turned out to be system independent. The resulting group occupancies are shown in parentheses in Table 3.

A water molecule in a certain group is allowed to form hydrogen bonds both with molecules within its own group and

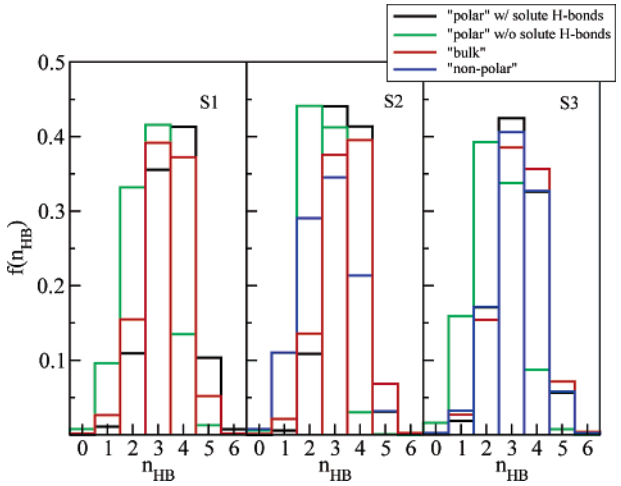

Figure 10. Fraction of water molecules from each of the three groups (polar, nonpolar, and bulk) participating in n_{HB} hydrogen bonds, in the S1−S3 systems for the octamer. Black line: polar water molecules and n_{HB} includes the bonds with the octamer. Green line: polar water molecules and n_{HB} does not include the bonds with the octamer. Blue line: nonpolar. Red line: bulk.

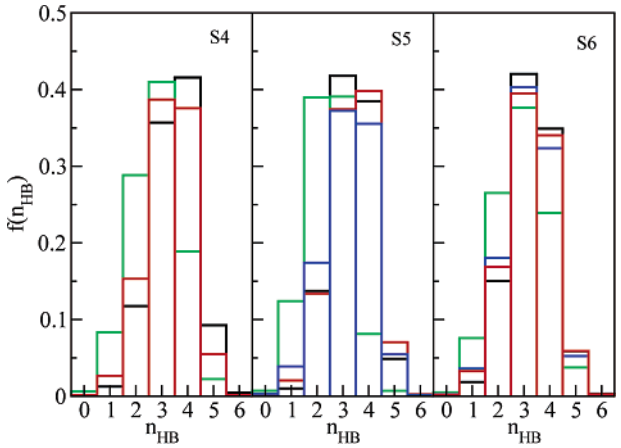

Figure 11. Same as in Figure 10 but for the hexamer systems, S4−S6.

Table 4. Average Number of Solvent Hydrogen Bonds Per Molecule in the Three Solvent Groups

system	S1	S2	S3	S4	S5	S6
polar w/solute	4.01	3.86	3.74	3.97	3.83	3.79
polar w/o solute	3.11	2.85	2.84	3.26	2.94	3.39
nonpolar		3.25	3.71		3.71	3.67
bulk	3.77	3.86	3.80	3.78	3.87	3.73

with molecules that belong to other groups. In addition, the polar water molecules are allowed to participate in hydrogen bonds with the oxygens (typically the terminal ones) in the polysilicate anions. In this study, we have adopted a geometric definition of the hydrogen bond, namely, the O−O distance is less than or equal to 3.5 Å and the H−O···O angle is less than or equal to 30°.[37] Histograms presenting the average fraction, f (n_{HB}), of water molecules that participate in n_{HB} hydrogen bonds are shown in Figures10 and 11. The average number of hydrogen bonds per molecule in each solvent group is given in Table 4.

To proceed with the analysis of the H-bond histograms, we should first make the observation that the bulk distribution remains practically the same across all systems, as it should be, because the bulk water molecules should not be influenced by the presence of the solute molecules. Only in the systems with high solute concentrations (S3 and S6) do we see a minor decrease in the fraction of four-bonded water molecules, also as expected. Overall, in the bulk group, we have approximately equal fractions of three- and four-bonded molecules (∼38−40%), ∼15% of two-bonded, and ∼5% of five-bonded molecules. These fractions are in excellent agreement with previous simulations of neat water.[37−39] In Table 4, we see that $\langle n_{HB}\rangle_{bulk}$ is, within statistical error, the same for all systems.

In the systems with TMA in solution (S2, S3 for the octamer [cf. Figure 10] and S5, S6 for the hexamer [cf. Figure 11]), the distribution $f(n_{HB})$ for the nonpolar group resembles that of the bulk, except in S2, where there is a substantial decrease in the fraction of four-bonded water molecules in favor of a higher fraction of two-bonded molecules. This results in a 16% decrease in $\langle n_{HB}\rangle_{nonpol}$ compared to the bulk (cf. Table 4), well above the statistical uncertainty of the computed averages (1−3%). Recall that S2 is the $Si_8O_{20}^{8-}$·8TMA complex and, in the course of the MD simulation, the TMAs were constrained at the surface of the silicate. In essence, the molecules in the nonpolar group belong to the first solvation shell of the hydrophobic cations. Typically, solvation of small hydrophobic solutes, like TMA, does not entail H-bond breaking; rather, the solvent can reorganize in order to preserve its H-bond network. Here, however, because the TMA molecules that have been constrained at the surface of the octamer are part of a bulky solute and, locally, the solvent fails to reorganize and maintain its network—a fraction of its hydrogen bonds has to break. In general, this is typical behavior near the surface of a bulky hydrophobic solute.[40] This is very important, because it shows that *TMA at the surface of the cubic octamer gives the latter partly hydrophobic character*. In contrast, we do not observe this behavior in the case of the $Si_6O_{15}^{6-}$·6TMA complex (S5), despite the fact that the 6 TMAs were constrained to remain at the surface.

The reader at this point may wonder, however, why do we not see in S3 behavior similar to that in S2. The answer is that in S3 the TMA cations were not constrained at the surface and, although we have found that, at this high TMA concentration, six TMA molecules coordinate around the cubic octamer,[3] the remaining 10 TMAs remain in solution and behave as one would have expected them to do—as small hydrophobic solutes. Thereby, in S3, the distribution $f(n_{HB})$ in the nonpolar group is dominated by the water molecules in the immediate vicinity of the TMAs that are in solution and not so much by those in the vicinity of the adsorbed TMAs. The same argument applies to the system S6, where we have seen that no TMA adsorption takes place (cf. section 3.A.), therefore, all 12 TMA molecules are in solution.

Excluding the H-bonds between water and the silicate solute, the distribution $f(n_{HB})$ of the number of hydrogen bonds per molecule in the polar group is shifted toward the smaller values of n_{HB}, in all the systems considered here. As a result, we see a significant decrease in $\langle n_{HB}\rangle_{pol}$, ranging between 9 and 26% relative to the bulk group (cf. Table 4). The smallest decrease relative to $\langle n_{HB}\rangle_{bulk}$ is observed for the hexamer systems S4 and

(37) Luzar, A.; Chandler, D. *Phys. Rev. Lett.* **1996**, *76*, 928−931.
(38) Luzar, A.; Chandler, D. *J. Chem. Phys.* **1993**, *98*, 8160−8173.
(39) Luzar, A.; Chandler, D. *Nature* **1996**, *379*, 55−57.
(40) Chandler, D. *Nature* **2002**, *417*, 491.

S6. Recall, however, that in these two cases the solvent classification was performed using an energy criterion and, as we noted earlier, the energy cutoffs that we used amounted, in essence, to substantially increased distance cutoffs in the spatial classification criterion. As a result, in S4 and S6, the water molecules in the polar group have a rather mixed "identity", with substantial bulk characteristics. When the hydrogen bonds with the silicate solute are included, the distribution shifts toward higher values of n_{HB} and becomes remarkably similar to that of molecules in the bulk group for all systems considered. As a result, the value of the average number of hydrogen $\langle n_{HB}\rangle_{pol}$ per molecule in the polar group is practically restored back to the bulk value.

Reviewing our findings from this subsection, we note the following: (i) The water molecules in the immediate vicinity of the hexamer are very mobile, and their hydrogen bonds with the silicate oxygen atoms appear to be very short-lived, unless the surface of the hexamer is fully covered with TMA. (ii) The surface of the octamer acquires hydrophobic character when TMA is adsorbed on it, a behavior not shared by the hexamer. (iii) A molecule in the immediate vicinity of the silicate solutes participates in fewer hydrogen bonds with other water molecules compared to the bulk, unless we count the hydrogen bonds with the solutes themselves. In the latter case, the average number of hydrogen bonds per water molecule in the polar group is equal to that in the bulk.

D. Water−Solute Hydrogen Bond Dynamics. In section 3.C., we saw that our attempt to classify the solvent molecules according to their time-averaged, spatial separation from the polar (silicate oxygens) functional components failed in the case of the silicate anion, Q_6^3, when there was no TMA adsorbed at its surface (systems S4 and S6). For the prescribed cutoff d_{cp} = 4.0 Å, and on account of the meaning of eqs 2 and 3, we argued that the procedure failed because, on the average, a water molecule does not spend a lot of time in the vicinity of the hexamer oxygen atoms and the corresponding hydrogen bonds are rather short-lived. We should, however, point out that a number of water molecules were labeled as polar in the case of the octamer, even when the latter was not fully covered with the organic cations. Although we do not believe that one should make much of the fact that the device of artificially classifying the solvent molecules into groups fails in some instances, it has nevertheless motivated us to investigate the issue a bit further since a clear distinction between the octamer and the hexamer has arisen, and it may very well have to do with solvent dynamics in conjunction with TMA adsorption at the surface of the silicate cages. To that end, for the systems considered here, we shall calculate the water−silicate hydrogen bond lifetime.

We shall calculate it from the time correlation function of the hydrogen bond occupation operator, h. For a tagged water−silicate oxygen pair, at any given time t, $h = 1$ when the pair is hydrogen bonded and $h = 0$ otherwise. For the hydrogen bond, we shall use the same configurational criterion as before. In the dynamical equilibrium of the solution, the hydrogen bond population operator fluctuates in time. These fluctuations are characterized by the correlation function

$$c(t) = \langle h(0)h(t)\rangle/\langle h\rangle \tag{8}$$

where $\langle h\rangle$ is the average number of hydrogen bonds. The function $c(t)$ has a simple interpretation; it gives us the probability that a hydrogen bond is still formed at time t given that it was intact at $t = 0$. In a large system, at equilibrium, the probability for a tagged pair to remain hydrogen bonded is negligibly small. Thereby, $c(t)$ relaxes to zero. The rate of relaxation to equilibrium is given by

$$k(t) = -dc/dt = \langle \dot{h}(0)h(t)\rangle/\langle h\rangle \tag{9}$$

where the dot denotes time derivative. The function $k(t)$ provides information about the short-time dynamics (i.e., transient relaxation), as well as the long-time dynamical relaxation and thereby the phenomenological rate constant.[41] In this article, we are interested in the latter. At times much longer than the transient relaxation time, if the macroscopic dynamical relaxation to equilibrium follows an exponential rate law, then the microscopically calculated $k(t)$ should plateau out. Thus, $k(t) \sim (1/\tau)\exp(-t/\tau)$ for $t \gg \tau_{mol}$, where τ_{mol} denotes the transient relaxation time.

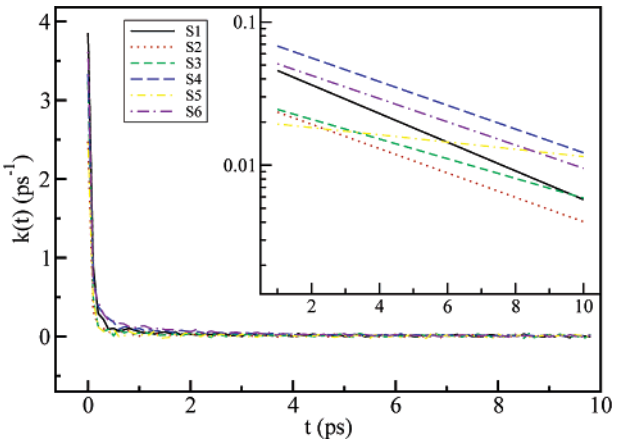

Figure 12. The rate of relaxation of the water−silicate hydrogen bond population operator time correlation function. In the inset, we show the exponential functions that were fitted to the plateau region of the functions $k(t)$.

The plateau value will then give us the rate at which a water molecule−silicate hydrogen bond breaks apart. In Figure 12, we show the functions $k(t)$ for the six systems examined. In all of them, $k(t)$ reaches a plateau after a transient time of about 0.5 ps. To obtain the phenomenological rate constant, an exponential function was fitted to the plateau region of $k(t)$. The rate constants are shown in Figure 13, and the corresponding lifetimes are shown in Table 5. For all the systems considered here, after equilibration, the present data for $k(t)$ were collected from 10 consecutive MD trajectories, each of 50 ps in length, except in S6, where each was 200 ps in length.

We discern clear trends. The S4 and S6 systems do indeed have the shortest water−silicate hydrogen bond lifetimes, 12.0 and 16.4 ps, respectively. In the case of the octamer in aqueous solution without TMA (S1), we observe the same behavior with τ_{HB} = 17.2 ps. It was thus quite fortuitous that the solvent classification procedure did not fail to put water molecules into the polar group in this case. For the S2 and S5 systems, in which the TMA molecules have been constrained at the surface of the octamer and hexamer, respectively, we obtain longer water−silicate H-bond lifetimes. Moreover, in the case of the S3 system, where the TMAs are not constrained at the surface and at

(41) Chandler, D. *Introduction to Modern Statistical Mechanics;* Oxford University Press: Oxford, 1987.

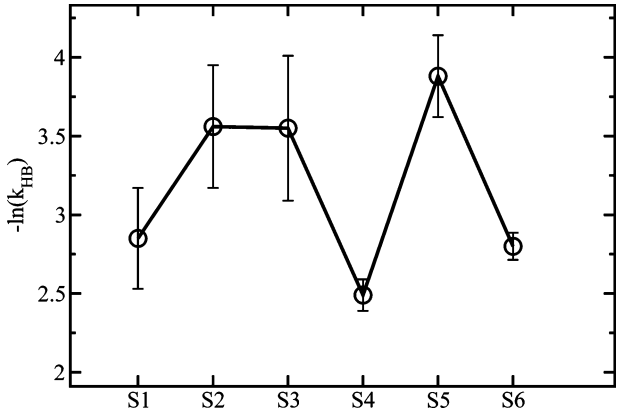

Figure 13. Rate constants for the breaking of a water molecule−silicate oxygen hydrogen bond computed from the time derivative of the time correlation function of the hydrogen bond occupation operator. (The line is drawn as a visual aid.)

Table 5. Average Lifetime for the Hydrogen Bond between a Water Molecule and a Silicate Anion Oxygen Atom in Systems, S1−S6

system	S1	S2	S3	S4	S5	S6
τ_{HB} (ps)	17.2	35.7	34.5	12.0	47.6	16.4

equilibrium six of them are coordinated around the octamer, the water−silicate hydrogen bond has practically the same lifetime as that in S2, in which the TMAs were not free to move.

Clearly, when the TMA molecules are forced to stay on the surface of the hexamer, then the hexamer−TMA complex behaves remarkably similar to the octamer−TMA complex. Moreover, it is evident that the presence of a TMA layer around the cage-like species Q_8^3 and Q_6^3 has a significant effect on the solvent dynamics in their vicinity—it increases the lifetime of the hydrogen bonds between the water molecules and the polysilicate anions. In the context of elucidating the function of tetraalkylammonium cations in the mechanism of zeolite formation, we believe that this is an important result. Silicate clathration, with concomitant TAA occlusion, has been speculated to be the very first step in the formation of precursor species prior to nucleation in zeolite crystal growth.[6−9] As we said earlier, for this to happen, SiO_2 units must replace water molecules in the TAA's hydration shell. As they do so, the SiO_2 units start to form small clusters, possibly of cage-like morphology similar to that of the octamer or the hexamer, that can act as precursor species in the nucleation process. Such a mechanism is bound to have an effect on solvent structure and dynamics in the immediate neighborhood of these species. Evidently, the stability of these small clathrates would depend on how stable the hydrogen bonds between the surrounding water and the silicate clusters are. We have seen here that the presence of TMA results in increased lifetime of these bonds.

4. Concluding Remarks

We have shown that, even at high TMA concentrations, the prismatic hexamer $Si_6O_{15}^{6-}$ cannot support a stable TMA layer around it, in stark contrast with the octamer. We have thus drawn a strong correlation between the stability of these two species and the ability of TMA to adsorb onto their surfaces. We believe that this correlation reinforces the theory that one of the roles of TMA is to *protect* the siloxane groups from hydrolysis by expelling water in the vicinity of the bridge oxygens.[1,2]

By calculating the free energy of formation of the Q_6^3·6TMA complex in the liquid phase, we have concluded that it cannot be characterized as an unstable species, but rather as a long-lived metastable state. By comparing it with the energy for the formation of the Q_8^3·8TMA complex, we have seen that the latter is more stable in aqueous solution by about 70 kcal/mol. This picture is consistent with experimental data according to which the hexamer forms in the beginning but over time disappears in favor of the octamer.

Owing primarily to their silanol oxygens, both species participate in hydrogen bonds with the water molecules. By dividing the solvent molecules into classes according to their local environment and proximity to the various functional groups of the solute species in solution, we have shown that the water molecules in the immediate vicinity of the polysilicate anions participate in fewer hydrogen bonds with neighboring water molecules, relative to those in the bulk. If, however, one includes the hydrogen bonds with the silicate solutes, then the average number of hydrogen bonds per molecule in the vicinity of the solute is roughly equal to that in the bulk. Remarkably, the presence of the cage-like anions in the solution does not appear to disturb the solvent hydrogen bond network. It would be difficult, however, to quantify this statement without carrying out explicit free energy calculations, which could provide entropic contributions to the solvation of these species. Such computational studies are currently underway.

Furthermore, we have seen that in the case of the octamer, the presence of a TMA layer around it results in the octamer surface acquiring characteristics typical of surfaces of large hydrophobic solutes. This is an important point, with significant ramifications regarding the way such species interact and/or aggregate. This point has often been overlooked, and the TAAs have been treated merely as counterions because of the net charge that they carry. However, our simulations indicate that the hydrophobic character of their alkyl chains should not be neglected, especially in the case of the higher TAAs.

Finally, by studying the dynamics of the hydrogen bonds between the water molecules and the polysilicate anions Q_8^3 and Q_6^3, we have shown that the presence of a TMA adsorption layer has a rather profound effect on these bonds—it increases their lifetime by at least a factor of 2. An immediate extension of this conclusion is that by increasing the stability of the hydrogen bonds between water and precursor silicate clusters, TAAs may facilitate clathrate formation. Although more studies will be needed in this direction to extend our findings to more silicate systems and larger TAAs and to place them on even firmer footing, we may claim that for the first time we have a glimpse into the admittedly complex role of TAAs in the synthesis of zeolites. It appears that this role goes beyond mere structure direction.

Acknowledgment. Funding for this work was provided by NSF/NIRT, CTS-0103010, and NSF, CTS-0312117. S.C. and D.G.V. gratefully acknowledge stimulating discussions with Professor Raul Lobo.

JA0561136